Experimental Investigation of Continuous Single-Phase Rimming Flow in a Horizontal Rotating Cylinder

Saravanan Suppiah Singaram and Himanshu Lodha
Dept. of Chemical and Biomolecular Engineering, Clarkson University, Potsdam, NY 13699

Roshan J. Jachuck
Dept. of Chemical and Biomolecular Engineering, Clarkson University, Potsdam, NY 13699

R3 Fusion Inc., Rensselaer Technology Park, Troy, NY 12180

DOI 10.1002/aic.14569
Published online August 6, 2014 in Wiley Online Library (wileyonlinelibrary.com)

Rimming flow of water that leads to a thin film onto the inner surface of a horizontally rotating cylinder is studied in this work. At higher rotational speeds, axial flow of uniform thin film is established inside the rotating cylinder. Film thickness measurements under different flow conditions were performed in the annular flow regime using an optical interferometric technique. Dimensional analysis was also performed to understand the parametric dependence of key parameters involved in the rimming flow of water inside a horizontal rotating cylinder and expressions to determine average film thickness and average residence time are also presented. This study will provide a basis to estimate the transport characteristics in the thin film inside the horizontal rotating cylinder. © 2014 American Institute of Chemical Engineers *AIChE J*, 60: 3939–3950, 2014
Keywords: coating flows, horizontal rotating cylinder, thin film flows, process intensification, transport

Introduction

In many industrial processes, chemicals are processed by spreading them as a thin film over a surface to achieve smaller path lengths for the transport processes. The mechanical devices that are used to spread and maintain the reactants in thin films are usually rotary devices because of the centrifugal force that can be used to spread the liquid over the solid surface. Some of the mechanical systems that are used to form a thin film include rotating cylinder (or drum), spinning disc reactor, rotating heat pipes, and so forth.

High heat transfer, mass transfer, and mixing rates can be achieved by having liquid flow in the form of a thin film along the inner surface of a horizontally rotating cylinder. This special type of coating flow that is established inside a rotating cylinder is typically called rimming flow[1–6] and can be exploited to develop reactors suitable for continuous flow operation.[7] These reactors may be used for applications such as pasteurization of milk,[8] evaporation of organic solvents from a mixture, production of nano-particles, biodiesel production,[9] and coating of sol–gel films.[10]

Single-phase rimming flow in a partially-filled horizontally rotating cylinder has been extensively studied by many researchers.[1–6] The cylinder is partially filled with liquid and rotated about the horizontal axis to establish coating flow. This mode of operation is referred to as "batch mode" in this work as there is no inflow or outflow of liquid during the experimental study. This type of coating flow offers different kinds of flow regimes (hydrodynamic regimes) based on the choice of parameters such as the aspect ratio of the cylinder, the choice of the liquid, fill fraction, and the rotational speed. At low rotational speeds, the film coalesces with the liquid pool at the bottom of the cylinder. This regime, which is referred to as "pool flow" regime, becomes unstable at higher rotational speeds and finally forms a thin film after a critical rotational speed is reached. The regime where it forms a homogenous thin film inside the cylinder after attaining a critical rotational speed is referred to as "annular flow" regime. A detailed description of different flow transitions that are encountered in rimming flow in a partially-filled horizontal rotating cylinder is given by Thoroddsen and Mahadevan.[5]

Rimming flow can also be established inside a horizontal rotating cylinder by continuously feeding the liquid at one end of the cylinder and collecting the liquid at the other end.[7–9,11–13] This mode of operation is referred to as "continuous mode" in this work as there is continuous inflow and outflow of liquid during the experimental study. The different flow regimes observed in the case of batch mode are also observed in continuous mode. In this work, continuous mode rimming flow is investigated to experimentally study the flow transitions that occur when different parameters such as liquid flow rate or rotational speed of the cylinder are varied. Figure 1 shows a metallic jacketed-rotating cylinder capable of creating rimming flow in a continuous flow configuration.

A major difference between flow in a batch system and a continuous system is that the volume of liquid inside the cylinder (liquid holdup) in a continuous system changes with

Correspondence concerning this article should be addressed to S. S. Singaram at saravanan.suppiah@ingredion.com.

© 2014 American Institute of Chemical Engineers

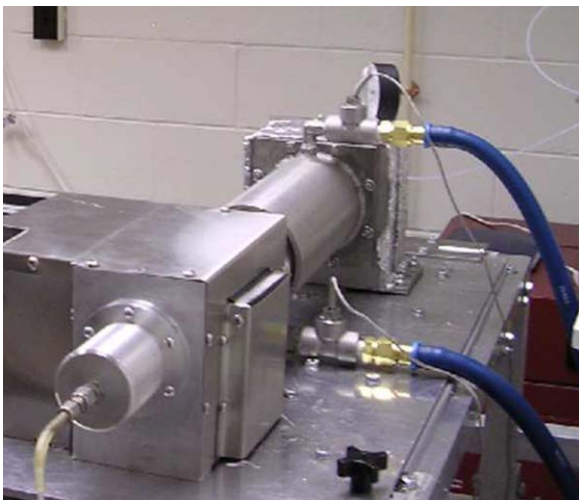

Figure 1. Photograph of a jacketed-rotating cylinder.

[Color figure can be viewed in the online issue, which is available at wileyonlinelibrary.com.]

rotational speed for any given flow rate and whereas in a batch system the liquid holdup remains the same for any particular fill fraction and only the local distribution of liquid varies with rotational speed. Also, unlike in experiments in a partially-filled cylinder, liquid holdup was not readily known as it depends on liquid properties such as density and viscosity and also other parameters such as flow rate, rotational speed, and the physical dimensions of the cylinder. However, the volume of liquid (at any flow rate and rotational speed) inside the cylinder could be assumed to be constant at steady state for any particular flow condition.

The main aim of our work is to investigate single-phase rimming flow in a horizontally rotating cylinder with a focus to experimentally measure liquid film thickness in the annular flow regime (shown in Figure 2d). Annular flow regime is of importance to the applications that involve thin film processing. Some of the applications that involve thin film processing are mentioned earlier. In the annular flow regime, average residence time of liquid inside the rotating cylinder can be calculated if the average liquid film thickness is known. The knowledge of film thickness in such a flow system will facilitate the prediction of transport rates for potential thin film processing applications that can be studied in a horizontal rotating cylinder. Hence, it is important to know the liquid film thickness under different flow conditions.

Literature and Background

The available experimental and theoretical studies on rimming flow focus on flow inside a partially-filled rotating horizontal cylinder. Most researchers have studied rimming flow analytically.[1–3,6] The experimental work on rimming flow mostly includes high viscosity liquids in partially-filled cylinders.[1,2,5,6] The main focus of these works was to investigate the flow transitions and the instabilities that occur during the flow. Yasmin et al.[13] has studied dynamic thin films formed inside a rapidly rotating tube open at one end at high rotational speeds for finite submillilitre volumes of liquid.

Hydrodynamic flow regimes

Phillips[3] and Baker et al.[4] used water as test liquid in their rimming flow studies inside a partially-filled horizontal rotating cylinders to investigate the collapse of annular flow to pool flow state. Phillips[3] analyzed the wave motion on the free surface of a rapidly rotating liquid inside the horizontal rotating cylinder. The motion was studied assuming small perturbations to a rigid rotation and a criterion for the stability of the motion was presented. The empty cylinder was rotated at a certain rotational speed and then water was added slowly to find the critical volume or fill fraction of water (which corresponds to a certain thickness of water layer) above which the homogenous film became unstable and collapsed suddenly. The stability criterion was given in terms of Froude number. Baker et al.[4] gave correlations of critical Froude numbers for the transition to annular flow when the rotational speed is increased from zero and for the collapse of the film to the pool flow state when the rotational speed is decreased after reaching the critical rotational speed at which annular flow occurs.

High viscosity fluids were studied by Moffatt[1] using lubrication theory. Melo[2] used silicone oil as the test fluid to experimentally study the existence domain of the annular flow regime for different fill volumes. Thoroddsen and Mahadevan[5] described the different flow modes displayed by rimming flow in detail. Phase diagrams showing the flow modes that occur at different rotational speeds as a function of different volume filling fractions of liquid inside the cylinder were given. The influence of viscosity was also studied in the range of 2–1020 mPa.s.

Liquid film thickness measurement

A thorough literature survey reveals that there is no available literature on rimming flow established with a continuous

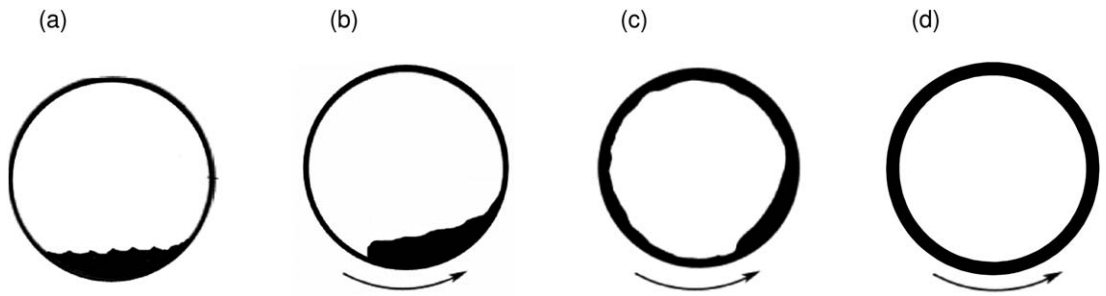

Figure 2. Cross-section of the cylinder showing liquid flowing out when cylinder is (a) stationary, (b) rotating at very low rotational speeds, (c) rotating at rotational speeds below the critical rotational speed for annular flow, resulting in pool flow with a thin film arising out of the pool at the bottom, and (d) rotating at higher rotational speeds above the critical rotational speed to achieve annular flow regime.

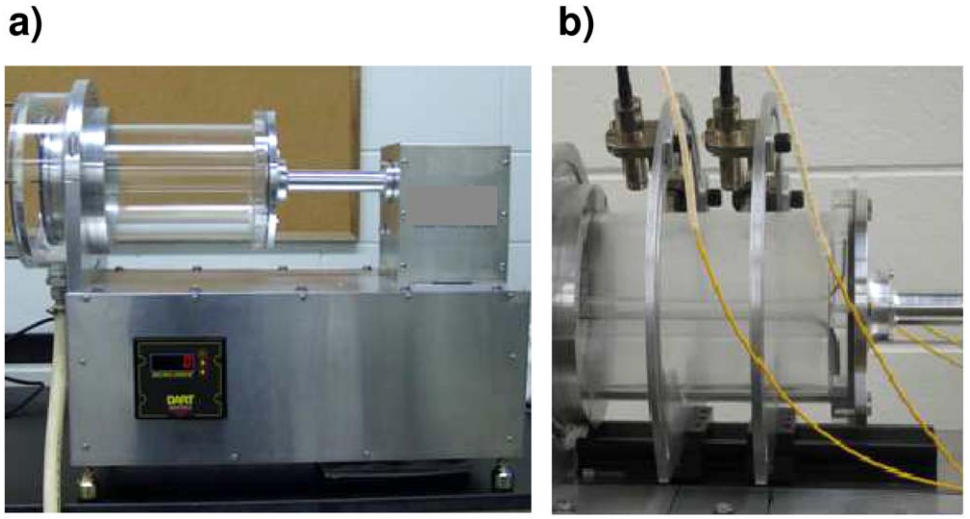

Figure 3. (a) Photograph of the cylinder and (b) Photograph of the cylinder shown with film thickness measurement probe assembly.

[Color figure can be viewed in the online issue, which is available at wileyonlinelibrary.com.]

inflow and outflow of liquid where film thickness measurements are reported except for a patent that describes a chemical process on the surface of a rotating body.[7] Cowen et al.[7] mentions that the rotational speeds used in their processes were in excess of 500 rpm and it was given that the forces operating on the liquid causing it to move depends on the physical dimensions of the rotating body. An expression for residence time t was given by Eq. 1

$$t = \left(\frac{6\pi R^2 \mu L^5}{Q^3 f^2 \rho}\right)^{1/4} \tag{1}$$

where, R and L are the radius and length of the rotating cylinder respectively, μ and ρ are viscosity and density of the liquid, respectively, Q is the liquid flow rate, and f is the rotational frequency of the cylinder.

Average film thickness $\bar{h}_{\text{Cowen}}$ was given to be

$$\bar{h}_{\text{Cowen}} = \left(\frac{Qt}{2\pi RL}\right) \tag{2}$$

Using Eq. 1 in Eq. 2 and using angular velocity $\omega = 2\pi f$, Eq. 2 can be rewritten as

$$\bar{h}_{\text{Cowen}} = \left(\frac{3}{2\pi}\right)^{1/4} \left(\frac{\mu QL}{\rho\omega^2 R^2}\right)^{1/4} = 0.831 \left(\frac{\mu QL}{\rho\omega^2 R^2}\right)^{1/4} \tag{3}$$

In the experimental studies conducted by other researchers in rimming flow inside partially-filled cylinders, the film thickness is measured using contact needles. The method of using contact needles is an invasive technique. Melo[2] measured local film thickness as a function of azimuthal angle in the annular flow regime using contact needles which had a precision of about 0.01 mm in radial direction and 0.2° in the angular direction. Tirumkudulu and Acrivos[6] have also used contact needles to measure liquid film thickness in their rimming flow studies. The needle gauge used had a precision of about 0.01 mm in radial direction and 2° in the angular direction.

The important criteria in the selection of a film thickness measurement technique are that it should be noninvasive and should have high precision. The ease of taking measurements at multiple locations (both in axial and angular directions) is another important factor. Annular flow occurs at higher rotational speeds and so when the cylinder is stopped, the liquid film collapses to become a pool at the bottom. If the measurement system needs to be housed inside the cylinder, the system will get wet and this will affect the subsequent measurements. Also, the operational flexibility is reduced if the measurement system needs to be placed inside in the cylinder. Most of the techniques available require that the measurement probe looks directly at the free surface of the film. These techniques will be suitable to measure film thickness in an open system than in an enclosed system like the one considered in this work.

A film thickness measurement system[14] developed by Lumetrics is used in this work for liquid film thickness measurements. The technique is based on optical interferometry. The most accurate methods of performing absolute distance measurements are based on optical interferometry. OptiGauge™ precision thickness measurement system is a robust all-fiber-based low coherence interferometer used to measure the absolute thickness of transparent artifacts. The system uses a high-precision fiber-optic interferometer which uses light reflections to provide extremely accurate and rapid measurement of multilayer coatings. The interferometer uses two light sources, a light emitting diode (LED) light source to produce reflections from surfaces and a second light source (laser) to accurately calibrate those reflections. The LED light source is a fiber-coupled superluminescent LED operating at a center wavelength of 1310 nm with a bandwidth of 50 nm. The coherent diode laser operates at a wavelength of 1552 nm. Optical thickness of the sample is measured by the system and if the index of refraction is known, the physical thickness of the sample can be calculated. The scan rate of the measurement system is typically 50 Hz. Accuracy of the measurement technique is 100 nm. Measurement reliability depends on the light intensity which in turn depends on how normal the interfaces are to the light that is being projected onto them. A detailed working principle of the measurement system is given in Badami et al.[14]

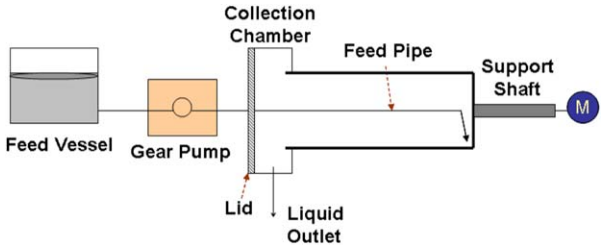

Figure 4. Schematic of the experimental setup.

[Color figure can be viewed in the online issue, which is available at wileyonlinelibrary.com.]

Experimental Setup

The experimental apparatus consisted of a hollow horizontal cylinder with inner radius and length of 7.6 and 29.7 cm, respectively. The cylinder was made of plexiglass (poly (methyl methacrylate)) and supported at one end by a solid shaft and the other end on a stationary frame using ball bearings with a mechanical seal. The wall thickness of the cylinder was 6.25 mm and had a tolerance of 1%. As the observed flow phenomena were found to be independent of the direction of rotation,[5] the direction of rotation was chosen to be anti-clockwise when viewed from the nondrive end side of the cylinder. Figure 3 shows the cylinder and also the film thickness measurement assembly with the probes.

Figure 4 shows the schematic of the experimental setup. Liquid feed vessel and the gear pump used to deliver the liquid can also be seen. The volumetric flow rate of liquid was maintained using a gear pump. The choice of gear pump was made to avoid pulsatile flow which is typical for peristaltic pumps. The inner diameter of the liquid feed pipe used was 4.1 mm (0.16 in.). The feed pipe could be seen in Figures 3b and 4. Liquid was introduced onto the inner wall at an angular position of 270° (pointing down in the direction of gravity; angular position was measured from the horizontal, see Figure 6) and at the drive-end side of the cylinder through a feed pipe that extends from the nondrive end side of the cylinder. The end where the liquid was introduced was closed with an end plate, and hence, the liquid was forced to flow toward the collection chamber at the other end. Liquid was collected at the outlet of the collection chamber at the other end as shown in Figure 4.

Liquid film thickness in the annular regime was measured using Lumetrics OptiGauge™ precision thickness measurement system. The measurement probes were housed in an annular ring assembly designed to hold the probes normal to the outer surface of the cylinder at the point of measurement. Figure 5 shows the annular ring assembly used to hold the optical probes. The assembly also facilitated the movement of probes in both angular and axial directions. Four probes were used to measure film thicknesses at two angular positions of 60° and 150° (shown in Figure 6) and two different axial positions of 4 and 7 in. from where the liquid was introduced (marked A and B in Figure 6). The choice of the angular positions was made to ensure that one of the measurements was done in the rising quadrant (where the liquid flows against the gravity) and the other in the falling quadrant (where gravity assists the flow).

Experimental Procedure

Deionized (DI) water was used as the test liquid in the experiments. The surface tension of water was measured

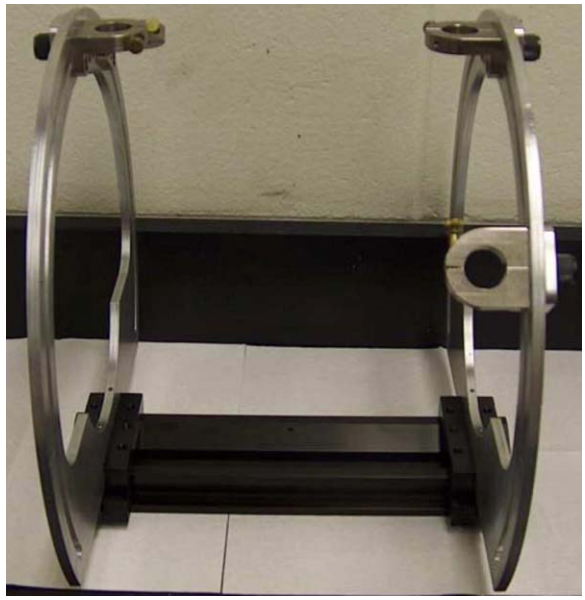

Figure 5. Annular ring assembly to hold the optical probes.

[Color figure can be viewed in the online issue, which is available at wileyonlinelibrary.com.]

using a ring-tensiometer (Fischer Surface Tensiomat) and the measured surface tension is 0.073 ± 0.002 N/m. The refractive index of liquid used is important in determining the physical thickness of the liquid film. The refractive index value of water reported in literature is typically at the incident light wavelength of 589 nm (refractive index at the Fraunhofer "D" line, the center of the yellow sodium double emission at 589.29 nm wavelength). As refractive index depends on temperature and wavelength of the light used, it is important to measure the refractive index using the same light source that is used in the measurement of optical thickness of the liquid film.

Liquid was charged in a cuvette of known physical path length and the interferometric system (wavelength of 1310 nm) was used to measure the optical path length of the incident light that is passed through the cuvette. As the physical path length of the cuvette is known, refractive index can be calculated using the equation given below[14]

$$\text{Refractive index} = \frac{\text{Optical Thickness}}{\text{Physical Thickness}} \tag{4}$$

Cuvettes with different path lengths of 1, 2, and 5 mm were used to calculate the refractive index of the liquid.[12] Optical thickness measurements were done at 22°C. The refractive index values obtained using different cuvettes are averaged and the average value of refractive index is 1.325 ± 0.001.

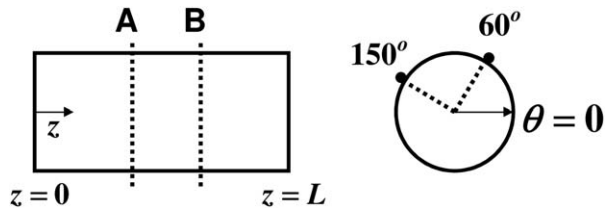

Figure 6. Schematic of the optical probe setup.

The experimental procedure for determining the hydrodynamic flow regimes and for measuring the liquid film thickness at different flow conditions are described below.

Hydrodynamic flow regimes

Experimental apparatus consisted of the cylinder described in the earlier section. A gear pump was used to feed water at flow rates between 4 and 11 mL/s. The choice of a gear pump was made to avoid pulsatile flow as pulsations in liquid feed would affect the hydrodynamic flow transitions in rimming flow, particularly the transition to annular film flow regime, and could destabilize the liquid film. Also, in these experiments, the level of liquid in the feed vessel did not affect the volume swept by the gear pump.

For any given liquid flow rate, rotational speed was varied slowly and in small increments (when approaching annular flow regime) or decrements (when approaching collapse of the annular film after the thin film was formed) to let the flow adjust to the new flow conditions. The waiting time between increments or decrements was approximately 40 periods of rotation and the typical increment or decrement size was 3 rpm. For a fixed flow rate, rotational speed plays an important role in determining the volume of liquid inside the rotating cylinder and also the film thickness in the annular film regime, unlike in a partially-filled cylinder (batch mode).

Experiments were performed to observe the flow phenomena and also to determine the critical rotational speeds corresponding to the onset of annular flow, complete annular flow, and the collapse of annular flow. The typical procedure is outlined below.

Liquid at a known volumetric flow rate was continuously fed onto the inner surface of the stationary cylinder using a gear pump. Rotational speed was increased slowly in small increments until annular flow was initially observed (onset). The rotational speed corresponding to the onset of annular flow was recorded. Rotational speed was further increased slowly until complete annular flow was observed. The rotational speed corresponding to complete annular flow was recorded. Once the complete annular flow state was reached, rotational speed was decreased slowly until the annular flow collapsed to "pool flow." The rotational speed corresponding to the collapse of annular flow was recorded. The procedure was repeated for different volumetric flow rates of the feed liquid.

Liquid film thickness measurement

The various parameters that are important in determining the liquid film thickness are liquid flow rate Q, cylinder angular velocity ω, liquid kinematic viscosity υ, radius of cylinder R, length of cylinder L, and the axial position z where thickness is determined. From the preliminary experiments, it was found that the film gets thinner along the axial length as it flows inside the cylinder and hence axial position where thickness is measured is also important in determining the film thickness. The effect of surface tension is not considered as it is found to have minimum effect[15] at higher angular velocities (annular flow regime) discussed in this work. Also, gravity forces are not considered at the higher angular velocities used in this work since Froude numbers (defined by $R\omega^2/g$, where g is acceleration due to gravity) were higher and were between 21 and 85 for the corresponding rotational speeds between 500 and 1000 rpm.

Film thickness h can be written as a function of the parameters that are considered above

$$h=F_1(Q,\omega,\upsilon,R,L,z) \tag{5}$$

Using kinematic viscosity of the liquid and radius of the cylinder to be the repeat variables, five dimensionless groups can be formed. The dimensionless groups obtained using Buckingham π theorem are given below

$$\Pi_1=\frac{h}{R} \tag{6}$$

$$\Pi_2=\frac{Q}{R\upsilon} \tag{7}$$

$$\Pi_3=\frac{\omega R^2}{\upsilon} \tag{8}$$

$$\Pi_4=\frac{L}{R} \tag{9}$$

$$\Pi_5=\frac{z}{R} \tag{10}$$

Using the above dimensionless groups, it can be written that

$$\Pi_1=F_2(\Pi_2,\Pi_3,\Pi_4,\Pi_5) \tag{11}$$

where Π_1 is a measure of liquid volume inside the cylinder, Π_2 is a measure of axial Reynolds number, Π_3 is a measure of rotational Reynolds number, Π_4 is dimensionless length, and Π_5 is dimensionless axial position where film thickness is determined. Equation 11 can be rewritten as

$$\frac{h}{R}=F_3\left(\frac{Q}{R\upsilon},\frac{\omega R^2}{\upsilon},\frac{L}{R},\frac{z}{R}\right) \tag{12}$$

As the length of the cylinder is not varied in this work, a new dimensionless group, $\left(\frac{L-z}{R}\right)$ is defined using the two dimensionless groups $\left(\frac{L}{R}\right)$ and $\left(\frac{z}{R}\right)$ and this new group is used as a measure of dimensionless axial position in this work

$$\Pi_6=\frac{L-z}{R} \tag{13}$$

The parameter $(L-z)$ is the axial distance from the liquid discharge end (outlet) where film thickness measurement is done. Equation 12 can be rewritten as

$$\frac{h}{R}=F_4\left(\frac{Q}{R\upsilon},\frac{\omega R^2}{\upsilon},\frac{L-z}{R}\right) \tag{14}$$

Each dimensionless group on the right-hand side of Eq. 14 is varied systematically, keeping the other dimensionless groups constant, to study the influence of that particular group on dimensionless liquid film thickness. The typical experimental procedure to measure liquid film thickness is outlined below.

In the first set of experiments, the ability of the interferometric system to measure the cylinder wall thickness, when the cylinder was stationary and when it was rotating, was evaluated. In the second set of measurements, the ability of the system to track solid–liquid interface was checked. These experiments were mainly done to check how the optical interferometric system used performs in tracking the interfaces as it primarily depends on the differences in indices of refraction. In the third set of experiments, the ability of the system to measure liquid film thicknesses was evaluated. In the fourth set of experiments, liquid flow rate and cylinder

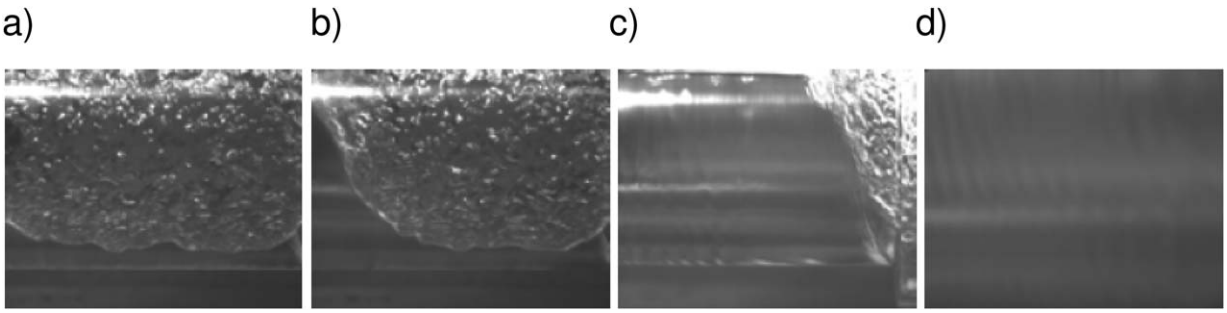

Figure 7. Side view of half the length of the cylinder when rotational speed is (a) just below the critical rotational speed for onset, (b) at the critical rotational speed for onset, (c) between the critical rotational speeds for onset and annular flow, and (d) above the critical rotational speed for annular flow regime; in the photographs shown, liquid flow direction is from right to left and the right most end is where the liquid is introduced.

rotational speed were fixed and film thickness measurements were done at two different angular and axial locations to qualitatively establish the spatial variation of thickness. In the fifth set of experiments, liquid flow rate and axial position where the thickness measurements were done were fixed and film thickness measurements were done at different rotational speeds of the cylinder. In the sixth set of experiments, cylinder rotational speed and axial position where the thickness measurements were done were fixed and film thickness measurements were done at different flow rates. In the last set of experiments, liquid flow rate and cylinder rotational speed were fixed. Axial position where the thickness measurements were done was varied (two such positions A and B are shown in Figure 6) and film thickness measurements were done at each axial position for the same flow conditions.

Experimental Results and Discussion

Flow phenomena—Hydrodynamic flow regimes

Study of flow phenomena in a batch flow system involves enclosing a certain fill volume of liquid in the cylinder and increasing the rotational speed from zero. A typical progression of flow phenomena observed in rimming flow of liquid inside a partially-filled cylinder has been described by Thoroddsen and Mahadevan.[5] Flow transitions from pool flow to annular thin film flow and then from annular thin film flow to collapse of the annular film were studied in a partially-filled cylinder by many authors. In this work, flow transitions in a rotating cylinder in which rimming flow is established in a continuous mode are studied.

For a given flow rate, the critical rotational speeds at which the transitions to different flow regimes occur were of primary interest. The typical flow phenomena observed at different flow rates of liquid inside the rotating cylinder is described below.

When the liquid at a known volumetric flow rate was continuously fed onto the inner surface of the stationary cylinder, the liquid flowed out of the cylinder forming a pool at the bottom of the cylinder. At lower rotational speeds, most of the liquid was at the bottom with a thin film arising out of the pool wetting the entire inner surface of the cylinder. Figure 7 shows some of the flow states observed. A "flat-front"[2] was created on the receding side of the cylinder (third quadrant) and an accompanying recirculating region at the bottom was also formed where the liquid film enters the liquid pool at the bottom (Figure 7a).

Sloshing was not observed for the flow rates studied (between 4 and 11 mL/s). The quantity of liquid dragged by the wall from the pool at the bottom at these flow rates was smaller than that for the fill volumes studied in batch conditions for which sloshing was observed by Thoroddsen and Mahadevan.[5]

The liquid film thickened with further increase in rotational speed (Figure 7c). The liquid front and the recirculation region disappeared gradually. After reaching a critical rotational speed for any particular flow rate, annular film started to form from the discharge end and travelled against the flow to nearly one fourth of the axial length from where the liquid was introduced (approximately one fourth of the cylinder length from the entrance). The transition to a state where there is a coexistence of a thin film region and liquid pool region along the axial length of the cylinder is referred to be "onset" of annular flow (Figure 7b). Figure 7 shows the different flow states observed when DI water was used as the test liquid.

Rotational speed was increased further to reach another critical rotational speed at which the liquid got homogenously distributed along the inner surface of the cylinder forming an annular film (Figure 7d). After reaching the critical rotational speed for complete annular flow, rotational speed was then decreased slowly. The annular film became unstable after reaching another critical rotational speed and the film collapsed in the direction opposite to the direction of rotation (backward breaking) to form a flat-front. This transition from annular flow to pool flow regime is referred to be "collapse" of the annular film. The rotational speed at which the liquid entered annular flow (when rotational speed was increased) was higher than the rotational speed at which it left annular flow (when rotational speed was decreased). This has been reported in literature for a batch system as "hysteresis." The difference between the critical rotational speeds for annular flow and collapse was found to increase when the flow rate was increased.

Figure 8 shows the parametric space for the existence of different flow regimes when DI water was used as the test liquid. Each reported critical rotational speed is an average value of five experimental measurements. When the experiments were repeated, collapse of the annular film occurred within 1 rpm of the reported average value and transition to annular flow regime occurred within 2 rpm of the average value.

Lines L1, L2, and L3 (shown in Figure 8) connect the corresponding critical rotational speeds at different flow rates for onset of annular flow, complete annular flow, and

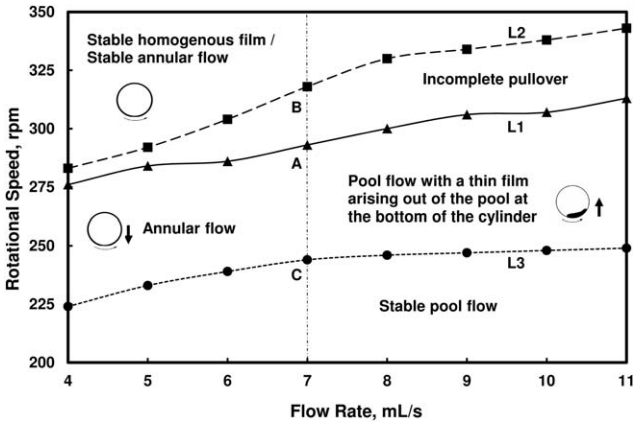

Figure 8. Parameter space for existence of different flow regimes; Lines L1, L2, and L3 are smooth lines drawn connecting the corresponding critical rotational speeds and not based on any model.

collapse of annular flow, respectively. Complete annular flow occurs in the region above the line L2. Between the lines L1 and L2, there is an "incomplete pull-over" of liquid to form annular flow and both pool flow and annular flow states coexist along the length of the cylinder. Below the line L3, pool flow occurs with a thin film arising out of the pool of liquid at the bottom. In the parameter space between the lines L3 and L2, the flow regime depends on how a particular rotational speed is attained for a fixed flow rate. For a flow rate of 7 mL/s (a reference line is shown in Figure 8), when the rotational speed is increased, onset of annular flow occurs at 293 rpm (Point A in Figure 8). If rotational speed is increased, complete annular flow occurs at 318 rpm (Point B in Figure 8). After reaching annular flow, if the rotational speed is decreased, collapse of the annular film occurs at 244 rpm (Point C in Figure 8). Between 244 and 293 rpm, the flow state could be either annular flow (if rotational speed is decreased after reaching annular flow) or pool flow (if rotational speed is increased from a collapsed or pool flow state) depending on how the rotational speed is attained. Also, the critical rotational speeds for different flow regimes strongly depend on the angular acceleration. Hence, the rotational speed was increased slowly as described earlier in the procedure.

Film thickness measurements

Film thickness measurements were done for different flow conditions at rotational speeds above the critical rotational speed for complete annular flow. As the probes were held stationary at a fixed position and the cylinder was rotating, 4000 measurements (sampling frequency of 50 Hz for 80 seconds) at each flow condition were taken to ensure that liquid film thickness measurement is not biased by the local wall thickness variation in the cylinder.

Evaluation of Film Thickness Measurement System. Optical thickness of the cylinder wall was measured using the optical interferometric system. The refractive index of the cylinder material used is 1.45. Using optical thickness values and refractive index, the physical thickness of the cylinder wall was calculated. The optical thickness measurements were taken at an axial distance of 8.5 cm from the end plate at the drive-end side of the cylinder and at an angular position of 150° (angular position is measured from the horizontal). The wall thickness of the cylinder according to the manufacturer is 6250 μm with a tolerance of 62.5 μm and the wall thickness values measured were between 6275 ± 23 μm. The wall thickness of the cylinder was also measured at different rotational speeds. The wall thicknesses measured were very close to the values obtained when the cylinder was stationary and only a weak dependence on rotation was observed.

Experiments were also done to test the capability of the system to track interfaces. Cylinder wall thickness measurements were done when there was no liquid flow inside the cylinder and when there was liquid flow at a flow rate of 10 mL/s. Liquid used was DI water. Measurements were taken at a cylinder rotational speed of 500 rpm. Optical probes were positioned at two axial locations of 10.2 cm (4 in.) and 17.8 cm (7 in.) and two angular positions of 60° and 150° at each axial position. Table 1 gives the cylinder wall thickness measurements at different locations. In Table 1, "Mean" is the average thickness value of 4000 measurements, "Std. Dev." is the standard deviation in wall thickness, and "99% CL" is the 99% confidence interval value for the mean thickness value. The optical interferometric system was able to locate the interface both when liquid was not flowing (solid-air interface to give the cylinder wall thickness) and when liquid was flowing (solid-liquid interface to give the cylinder wall thickness) inside the cylinder. For all probe locations where wall thickness measurements were done, the interface was located within 10 microns. In other words, the optical measurement technique could detect the difference in indices of refraction between the liquid used and cylinder material (PMMA) to give the wall thickness of the cylinder.

The measurement system was also evaluated for its capability to measure liquid film thicknesses. The cylinder outlet was closed with a lid and was filled partially with 2.5% of the total volume. The cylinder was rotated at different rotational speeds above the critical rotational speed to form a uniform thin film. If the film is considered to be spatially uniform, then the liquid film thickness should be 1010 μm for the amount of liquid filled inside the cylinder. The

Table 1. Cylinder Wall Thickness Measurements at Different Axial and Angular Locations in the Absence and Presence of Liquid Flow

Probe Location		Solid-Air Interface			Solid-Liquid Interface		
Axial (cm)	Radial (degrees)	Mean (μm)	Std. Dev. (μm)	99% CL (μm)	Mean (μm)	Std. Dev. (μm)	99% CL (μm)
10.2	60	6287	53	3.7	6289	54	3.1
10.2	150	6284	53	3.3	6287	54	3.1
17.8	60	6277	64	3.8	6284	63	3.7
17.8	150	6279	62	2.6	6285	63	3.7

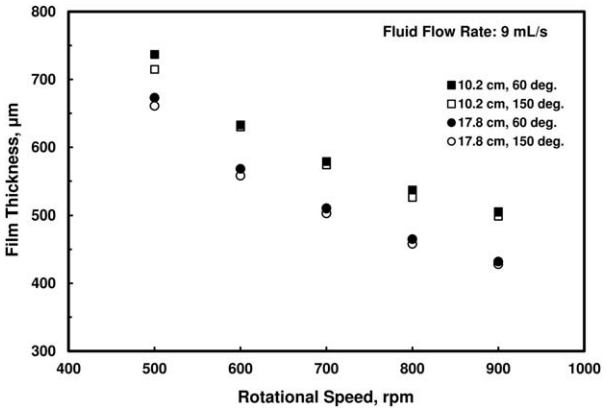

Figure 9. Spatial variation of film thickness for a flow rate of 9 mL/s; film thickness values shown are at axial positions of 10.2 and 17.8 cm from where the liquid feed is introduced and angular positions of 60° and 150°.

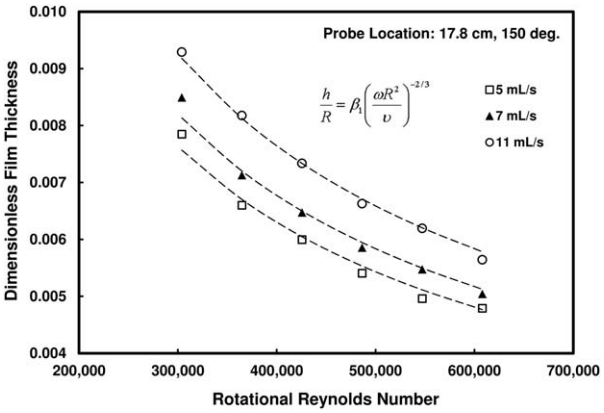

Figure 11. Variation of dimensionless film thickness with rotational Reynolds number for liquid flow rates of 5, 7, and 11 mL/s; film thickness values shown are at an axial position of 17.8 cm from where the liquid feed is introduced and an angular position of 150°.

measured film thicknesses were around 1030 μm with a standard deviation of 5 μm. The measurements were done at different axial and angular locations and the chosen axial locations were at least 5 cm from the end plates on both the sides to avoid edge effects. Given the local variation of film thicknesses, it can be said that the measurement system was able to measure liquid film thicknesses quite well.

Spatial Variation of Film Thickness. Liquid film thickness measurements were done at rotational speeds well above the critical rotational speeds for annular flow for the different flow conditions studied. The cylinder was started from rest and the rotational speed was increased to 300 rpm. Fluid at a fixed flow rate was continuously fed onto the inner surface of the cylinder. Rotational speed was increased slowly from 300 to 400 rpm. Measurements were taken at different rotational speeds between 400 and 1000 rpm with an increment of 100 rpm by slowly increasing the rotational speed.

Figure 9 shows liquid film thickness values at a liquid flow rate of 9 mL/s at different rotational speeds. Measurements were made at two axial positions of 10.2 and 17.8 cm and two angular positions of 60° and 150° for each axial position. Each experimental data value shown is an average value of five experimental observations. The experiments are highly reproducible with in ±5 μm in the annular flow regime (rotational speeds in excess of 500 rpm). It can be seen from Figure 9 that film thickness decreases with increase in the axial distance along the length of the cylinder from where the liquid was introduced. It can also be seen that film thickness variation in angular direction for any axial position decreases with increase in rotational speed. In other words, the liquid film becomes uniform in angular direction with increasing rotational speed and also with increasing axial distance in the flow direction. The decrease in liquid film thickness in the axial direction suggests that the liquid film accelerates in the flow direction.

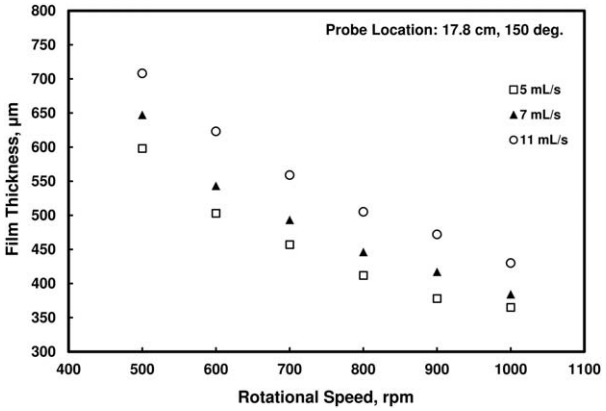

Figure 10. Influence of rotational speed on film thickness for liquid flow rates of 5, 7, and 11 mL/s; film thickness values shown are at an axial position of 17.8 cm from where the liquid feed is introduced and an angular position of 150°.

Influence of Rotational Speed. The cylinder was started from rest and the rotational speed was increased to 300 rpm. Liquid was introduced onto the rotating surface at a fixed flow rate and allowed to flow toward the discharge (from the drive end to the nondrive end side). Liquid flow rates studied were between 4 and 11 mL/s. Liquid film thickness measurements were performed at different rotational speeds between 400 and 1000 rpm by slowly increasing the rotational speed. At each chosen rotational speed, film thickness value obtained is a time-averaged value of 4000 measurements. Figure 10 shows the influence of rotational speed on film thickness for the flow rates of 5, 7, and 11 mL/s. It can be seen from Figure 10 that film thickness decreases with increase in rotational speed for all flow rates and increases with increase in flow rate for any particular rotational speed. The film thickness values measured were between 300 and 1000 μm for the range of flow rates and rotational speeds studied. Film thickness values were measured at an axial position of 17.8 cm from where the liquid was introduced and an angular position of 150°.

Experiments were repeated four times and the average value for liquid film thickness for each condition is reported in Figure 10. The standard deviation for each value reported is less than ±5 μm and the 95% confidence interval value is less than 8 μm.

Using the data in Figure 10, Figure 11 shows the variation of dimensionless film thickness (defined by Eq. 6) with a

Table 2. Values of β_1 and R^2 for the Different Flow Rates Studied

Flow Rate (mL/s)	β_1	$\mathbf{R}^2$
5	34.19	0.9803
7	36.74	0.9809
11	41.46	0.9955

dimensionless number referred to as rotational Reynolds number (defined by Eq. 8). When a power function by the form given in Eq. 15 is used to fit the experimental data, the exponent is found to be approximately -0.73, -0.74, and -0.71 for the cases when the flow rate is 5, 7, and 11 mL/s, respectively

$$\frac{h}{R}=\beta_1\left(\frac{\omega R^2}{\upsilon}\right)^{\xi_1} \tag{15}$$

For convenience and ease of obtaining a simple expression for dimensionless film thickness, the value of exponent was fixed to be $-2/3$ for each of the flow rates and the fit parameter β_1 was obtained by linear regression. The values of β_1 and $\mathbf{R}^2$ are given in Table 2 for the different flow rates studied.

Influence of Liquid Flow Rate. The cylinder was started from rest and the rotational speed was increased to 300 rpm and the liquid feed was introduced at 4 mL/s. The rotational speed was then increased to 600 rpm and maintained constant. Liquid film thickness measurements were taken for different flow rates between 4 and 11 mL/s (in increments of 1 mL/s) to study the influence of flow rate on film thickness. Film thickness values were measured at an axial position of 17.8 cm from where the liquid was introduced and an angular position of 150°. Figure 12 shows the influence of flow rate on film thickness for the rotational speed of 600 rpm. The choice of 600 rpm for rotational speed was made to make sure that the film was uniform in angular direction. Experiments were repeated three times and the average value for liquid film thickness for each condition is used. The standard deviation for each value reported is less than ± 2 μm and the 95% confidence interval value is less than 6 μm.

It can be seen from Figure 12 that film thickness increases with flow rate for all rotational speeds. For the flow rate of 7 mL/s, film thickness value obtained using the procedure described in this section is 533 μm and film thickness value obtained using the procedure described in the previous section is 543 μm. Hence, it can be said that reasonably similar film thickness values can be obtained irrespective of the path adopted to reach any particular parametric condition.

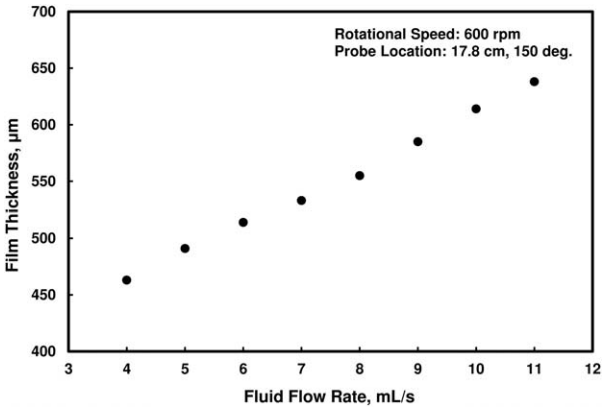

Figure 12. Influence of flow rate on film thickness for a cylinder rotational speed of 600 rpm; film thickness values shown are at an axial position of 17.8 cm from where the liquid feed is introduced and an angular position of 150°.

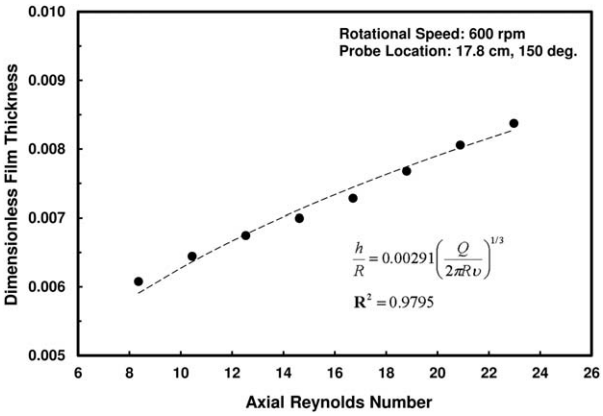

Figure 13. Variation of dimensionless film thickness with axial Reynolds number for a cylinder rotational speed of 600 rpm; film thickness values shown are at an axial position of 17.8 cm from where the liquid feed is introduced and an angular position of 150°.

Using the data in Figure 12, Figure 13 shows the variation of dimensionless film thickness with a dimensionless number referred to as axial Reynolds number. Axial Reynolds number is defined using the dimensionless group Π_2 and is given by Eq. 16.

$$\text{Axial Reynolds number} \equiv \frac{Q}{2\pi R\upsilon} \tag{16}$$

When a power function by the form given in Eq. 17 is used to fit the experimental data, the exponent is found to be 0.32

$$\frac{h}{R}=\beta_2\left(\frac{Q}{2\pi R\upsilon}\right)^{\xi_2} \tag{17}$$

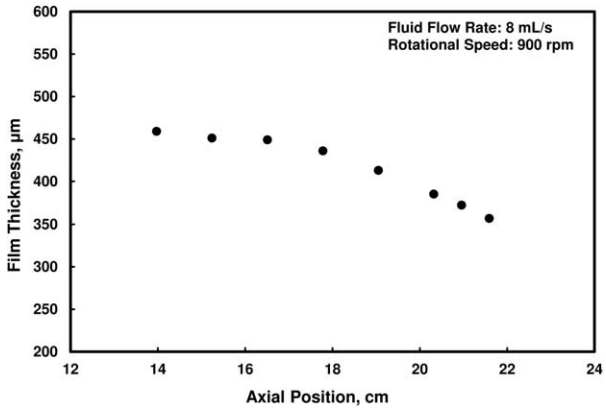

Figure 14. Variation of film thickness along axial position for a liquid flow rate of 8 mL/s and cylinder rotational speed of 900 rpm; film thickness values shown are at an angular position of 150°.

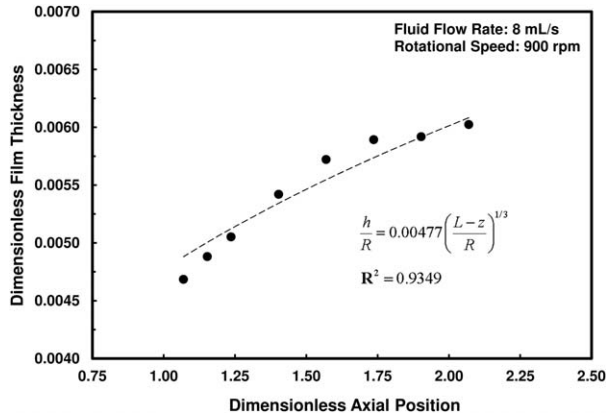

Figure 15. Variation of dimensionless film thickness with dimensionless axial position for a liquid flow rate of 8 mL/s and cylinder rotational speed of 900 rpm; film thickness values shown are at an angular position of 150°.

Again, for convenience and ease of obtaining a simple expression for dimensionless film thickness, the value of exponent was fixed to be 1/3 and the fit parameter β_2 was obtained by linear regression. The value of β_2 and $\mathbf{R}^2$ are 0.00291 and 0.9795, respectively.

Influence of Axial Position. The cylinder was started from rest and the rotational speed was increased to 300 rpm. Liquid was introduced onto the rotating surface at a fixed flow rate and allowed to flow toward the discharge. The rotational speed was then increased to 900 rpm. Rotational speed of 900 rpm was chosen to ensure that the film was uniform in angular direction for all flow conditions studied. At the fixed rotational speed of 900 rpm and a fixed flow rate, liquid film thickness measurements were taken at different axial positions between 10 and 22 cm by moving the annular ring assembly that holds the probes. Axial position is the distance from the location where the liquid was introduced. The length of the cylinder is 29.74 cm. Film thickness value obtained is a time-averaged value of 4000 measurements. Figure 14 shows the variation of film thickness along the axial length of the cylinder for liquid flow rates of 8 mL/s. It can be seen from Figure 14 that film thickness decreases with increase in axial position.

Experiments were repeated three times and the average value for liquid film thickness for each condition is reported in the figures. The standard deviation for each value reported is less than $\pm$ 4 μm and the 99% confidence interval value is less than 10 μm.

Figure 15 shows the variation of dimensionless film thickness with a dimensionless number referred to as dimensionless axial position $\left(\frac{L-z}{R}\right)$, where z is the axial position at which film thickness measurement was done and $(L-z)$ is axial distance from the liquid discharge (outlet) end at which film thickness measurement was done.

When a power function by the form given in Eq. 18 is used to fit the experimental data, the exponent is found to be 0.38

$$\frac{h}{R}=\beta_3\left(\frac{L-z}{R}\right)^{\xi_3} \tag{18}$$

The value of exponent was fixed to be 1/3 and the fit parameter β_3 was obtained by linear regression. The value of β_3 and $\mathbf{R}^2$ are 0.00477 and 0.9349, respectively.

Dimensional Scaling Analysis. It was shown that dimensionless film thickness, given by h/R, obeys to a power law with the three dimensionless numbers—rotational Reynolds number, axial Reynolds number, and dimensionless axial position

$$\frac{h}{R}=F_5\left(\frac{\omega R^2}{\upsilon},\frac{Q}{2\pi R\upsilon},\frac{L-z}{R}\right) \tag{19}$$

If we assume that the dimensionless film thickness is represented by a simple product form of the power functions (given by Eqs. 15, 17, and 18), then Eq. 19 can be written as

$$\frac{h}{R}=\beta\left(\frac{\omega R^2}{\upsilon}\right)^{\xi_1}\left(\frac{Q}{2\pi R\upsilon}\right)^{\xi_2}\left(\frac{L-z}{R}\right)^{\xi_3} \tag{20}$$

In Eq. 20, the values of ξ_1, ξ_2, and ξ_3 are chosen in the previous section to be $-2/3$, 1/3, and 1/3, respectively, and β is a constant

$$\frac{h}{R}=\beta\left(\frac{\omega R^2}{\upsilon}\right)^{-2/3}\left(\frac{Q}{2\pi R\upsilon}\right)^{1/3}\left(\frac{L-z}{R}\right)^{1/3} \tag{21}$$

Equation 21 can be rearranged as

$$\frac{h}{R}=\beta\left[\left(\frac{\upsilon}{\omega R^2}\right)^2\left(\frac{Q}{2\pi R\upsilon}\right)\left(\frac{L-z}{R}\right)\right]^{1/3} \tag{22}$$

$$\frac{h}{R}=\beta\left[\frac{\mu Q(L-z)}{2\pi\rho R^6\omega^2}\right]^{1/3} \tag{23}$$

Using all the experimental data, dimensionless film thickness, given by h/R, and the parameter $\left[\frac{\mu Q(L-z)}{2\pi\rho R^6\omega^2}\right]^{1/3}$ were calculated. Figure 16 shows that dimensionless film thickness varies linearly with the parameter $\left[\frac{\mu Q(L-z)}{2\pi\rho R^6\omega^2}\right]^{1/3}$. A linear fit for the experimental data gives a slope of 12.45 and a $\mathbf{R}^2$ value of 0.9362

$$\frac{h}{R}=12.45\left[\frac{\mu Q(L-z)}{2\pi\rho R^6\omega^2}\right]^{1/3} \tag{24}$$

$$h=\left(\frac{6.75}{R}\right)\left[\frac{\mu Q(L-z)}{\rho\omega^2}\right]^{1/3} \tag{25}$$

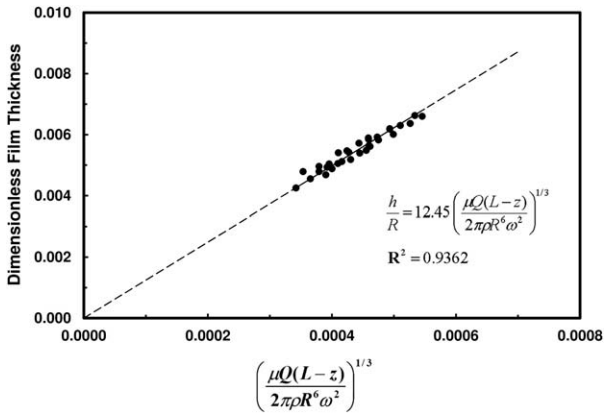

Figure 16. Variation of dimensionless film thickness with the parameter $\left[\frac{\mu Q(L-z)}{2\pi\rho R^6\omega^2}\right]^{1/3}$.

The above correlation obtained using dimensional analysis can be used in the case of water (or fluids with water-like viscosities) to predict the film thickness under different flow conditions. The correlation is validated for axial Reynolds number (defined by Eq. 16) between 8 and 23 and rotational Reynolds number (defined by Eq. 8) between 304,016 and 608,031. It should be used to predict film thicknesses for dimensionless axial position (defined by Eq. 13) between 1.0 and 2.1. It should be noted that Eq. 25 is only approximate and should be used well within the boundaries of the flow domain. This correlation will predict an incorrect film thickness value of zero when applied at the outlet of the cylinder ($z=L$). But, it can be said that the liquid film thins down in the axial flow direction and hence the liquid film can be viewed as accelerating in the axial direction. Also, it would be more meaningful to calculate an average film thickness value using Eq. 25. Average film thickness $\bar{h}$ can be defined by Eq. 26

$$\bar{h} \equiv \frac{\int_0^L h(z)dz}{\int_0^L dz} \tag{26}$$

$$\bar{h} = \left(\frac{1}{L}\right)\left(\frac{6.75}{R}\right)\int_0^L \left[\frac{\mu Q(L-z)}{\rho\omega^2}\right]^{1/3} dz \tag{27}$$

$$\bar{h} = \left(\frac{5.06}{R}\right)\left(\frac{\mu QL}{\rho\omega^2}\right)^{1/3} \tag{28}$$

Average film thickness values calculated from Eq. 28 can be compared with values from Eq. 3 given by Cowen et al. It can be seen that for the set of conditions used in this work, Eq. 3 under predicts the average film thickness. While Cowen et al. has also used Eq. 3 to predict film thickness values for fluids with viscosities higher than that for water, this study is done mainly with water as the test liquid.

Using Eq. 28, average velocity $\bar{v}$ and average residence time τ can be determined by Eqs. 29 and 30

$$\bar{v} = \frac{Q}{2\pi R\bar{h}} \tag{29}$$

$$\tau = L\bar{v} = \frac{2\pi R\bar{h}L}{Q} \tag{30}$$

In Eq. 30, the quantity $2\pi R\bar{h}L$ is the liquid hold-up volume inside the cylinder. Although Cowen et al. were able to predict the average film thickness and average residence time reasonably well, the variation of film thickness along the axial length was not addressed. The experimental work done in this study has clearly brought out the flow characteristics of the thin film flowing inside a rotating cylinder.

Conclusions

Rimming flow of water that is established in a continuous flow mode in a horizontal rotating cylinder was experimentally investigated. Flow phenomena observed were found to be similar to those typically observed in rimming flow inside a partially-filled cylinder. An optical interferometric technique was validated and used to measure liquid film thickness in the annular flow regime. Film thickness measurements in the annular flow regime are reported for the first time in a system, where rimming flow is established in a continuous flow mode.

It was found that the liquid film becomes more uniform in azimuthal direction with increase in rotational speed and also with the increase in axial distance from the feed entrance. Film thickness was found to decrease with increase in rotational speed for a given flow rate and increase with increase in flow rate for a given rotational speed. It has also been observed that for any given flow condition, the liquid film decreases along the axial length in the flow direction. If the liquid is considered to be uniform in the azimuthal direction, then it can be said that the liquid annular film accelerates as it flows down from one end of the cylinder to the other. It has been shown that different film thickness profiles can be obtained based on the operating parameters such as flow rate and rotational speed.

Correlations based on dimensional scaling analysis is also presented and based on the parameters considered, three different dimensionless groups were identified to influence the annular liquid film thickness. Liquid film thickness values can be used to determine the liquid hold up and average residence time of liquid inside the rotating cylinder.

Thin film contacting devices with thin liquid annular film flow can be designed based on the liquid film thickness values obtained in this work. These devices can be used for different applications that could involve reactions and separations. Some of the applications are biodiesel production, pasteurization of milk, particle production and coating, and evaporation of solvent. High pressure and vacuum processing can also be done in these types of thin film contacting devices. In this regard, this work will provide a basis to estimate the transport characteristics in the thin liquid film inside the horizontal rotating cylinder and will be useful in scale-up of rotating cylinders for different applications. Residence time and film thickness can be tuned for a specific application by varying parameters such as liquid flow rate, cylinder rotational speed, length, and diameter of the cylinder.

The flow transitions that occur at different critical rotational speeds could be studied in detail and a theory could be developed to predict these flow transitions. A study could be conducted to determine the film stability and breakup under different flow conditions. The influence of surface properties of the cylinder on flow transitions and thin film formation can be studied. Also, experiments could be performed with other low viscosity fluids to study the influence of flow parameters on film thickness and a theoretical model could be developed to understand the continuous flow characteristics of thin film inside a horizontally rotating cylinder. Finite element and computational fluid dynamics (CFD) models can be developed to study the flow transitions under different flow conditions and determine liquid film thickness values under different flow conditions in the annular flow regime. Multiphase flows can also be studied in a horizontally rotating cylinder that is setup in a continuous mode to understand the flow transitions under different flow conditions.

Acknowledgments

This work was performed while Dr. Saravanan Suppiah Singaram and Himanshu Lodha were students and Dr. Roshan Jachuck was a professor at Clarkson University. The authors thank Clarkson University for providing the

infrastructure and other necessities for supporting the research. The authors also thank Annapriya Thiagarajan for numerous helpful discussions.

Notation

f = Rotational frequency of the cylinder, 1/s
F_i = Parametric function
g = Acceleration due to gravity, m/s^2
h = Liquid film thickness, microns
$\overline{h}$ = Average liquid film thickness, microns
L = Length of the cylinder, cm
Q = Liquid flow rate, mL/s
R = Radius of the cylinder, cm
$\mathbf{R}^2$ = Regression coefficient
t = Residence time, s
$\bar{v}$ = Average velocity, cm/s
z = Axial distance from where the liquid is introduced, cm

Greek letters

β_i = Correlation fit parameter
μ = Dynamic viscosity, mPas
Π_i = Dimensionless group
ρ = Density of the liquid, g/cm^3
τ = Average residence time, s
υ = Kinematic viscosity, cm^2/s
ω = Angular velocity, rad/s
ξ_i = Correlation exponent

Subscripts

Cowen = expression given by Cowen et al.
i = Index value (= 1, 2, 3,...)

Literature Cited

1. Moffatt HK. Behaviour of a viscous film on the outer surface of a rotating cylinder. *J Mec*. 1977;16:651–673.
2. Melo F. Localized states in film-dragging experiments. *Phys Rev E*. 1993;48:2704–2712.
3. Phillips OM. Centrifugal waves. *J Fluid Mech*. 1960;7:340–352.
4. Baker J, Oliver T, Lin L, Ponnapan R, Leland J. Correlations of critical Froude number for annular-rimming flow in rotating heat pipes. *J Fluids Eng*. 2001;123:909–913.
5. Thoroddsen ST, Mahadevan L. Experimental study of coating flows in a partially-filled horizontally rotating cylinder. *Exp Fluids*. 1997; 23:1–13.
6. Tirumkudulu M, Acrivos A. Coating flows within a rotating horizontal cylinder: lubrication analysis, numerical computations, and experimental measurements. *Phys Fluids*. 2001;13:14–19.
7. Cowen G, Norton-Berry P, Steel ML. Chemical process on the surface of a rotating body. US Patent 4,311,570, 1982.
8. Suppiah Singaram S, Jachuck R. Development of Process Intensification Technology for the Food Processing Industry. NYSERDA Final Project Report, 2006.
9. Lodha H, Jachuck R, Suppiah Singaram S. Intensified biodiesel production using rotating tube reactor. *Energy Fuels*. 2012;26:7037–7040.
10. Christoph D, Christopher CW, Alexander AC, Sung HK, Marcus AW, Tom B, Stuart AG, Joe HS, Kuang JW, Alex VH, Juergen B. Coating functional sol–gel films inside horizontally-rotating cylinders by rimming flow/state. *J Sol-Gel Sci Technol*. 2013;65:170–177.
11. Suppiah Singaram S, Jachuck R. Single-phase rimming flow in a horizontal rotating cylinder. In: Muir A, editor. Green Chemistry & Engineering: International Conference on Process Intensification & Nanotechnology, Albany, New York, USA: BHR Group, 2008:93–101.
12. Suppiah Singaram S. Continuous single-phase rimming flow in a horizontal rotating cylinder. PhD thesis, Clarkson University, 2010.
13. Yasmin L, Chen X, Stubbs KA, Raston CL. Optimising a vortex fluidic device for controlling chemical reactivity and selectivity. *Sci Rep*. 2013;3:2282.
14. Badami, Vivek G, Blalock T. Uncertainty evaluation of a fiber-based interferometer for the measurement of absolute dimensions. *Proc SPIE*. 2005;5879:23–41.
15. Ashmore J, Hosoi EG, Stone HA. The effect of surface tension on rimming flows in a partially filled rotating cylinder. *J Fluid Mech*. 2003;479:65–98.

Manuscript received Sep. 19, 2013, and revision received June 1, 2014.